Activated mechanisms in amorphous silicon: An activation-relaxation-technique study

Normand Mousseau*

Department of Physics and Astronomy and Condensed Matter and Surface Science Program, Ohio University, Athens, Ohio 45701

G. T. Barkema[†]

Theoretical Physics, Utrecht University, Princetonplein 5, 3584 CC Utrecht, The Netherlands
(Received 27 May 1999)

At low temperatures, dynamics in amorphous silicon occurs through a sequence of discrete activated events that locally reorganize the topological network. Using the activation-relaxation technique, a database containing over 8000 such events is generated, and the events are analyzed with respect to their energy barrier and asymmetry, displacement and volume expansion/contraction. Special attention is paid to those events corresponding to diffusing coordination defects. The energetics is not clearly correlated with the displacement, nor with the defect density in well-relaxed configurations. We find however some correlation with the local volume expansion: it tends to increase by about 4 eV/Å^3. The topological properties of these events are also studied; they show an unexpectedly rich diversity.

I. INTRODUCTION

The properties of amorphous semiconductors can vary widely as a function of the details of the preparation method: hot-wire, electron-beam deposition,[1] and ion bombardment[2] can yield samples with a significant spread in electronic and structural properties. Such diversity is a reflection of the immensely large number of metastable configurations of nearby energy.

The topological structure of this complex energy surface can be sampled indirectly, for instance by light illumination or ion bombardment, bringing a sample from one metastable state to another, often in a (statistically) reversible manner. A direct study of this energy surface requires the identification at the microscopic level of the mechanisms responsible for moving from one metastable state to another, and is much harder to perform. Because of the high degree of disorder, very few techniques can provide a truly microscopic representation of the bulk dynamics.[3] At best, one can extract some quantity averaged in time and space, providing a very rough picture of what is really happening.

In spite of these difficulties, the past few years have seen significant experimental and theoretical efforts to try to provide some insight into the bulk dynamics. As it is becoming evident that little hard and precise information about the local environment can be obtained by via static methods, more and more emphasis is put onto the development of techniques to sample dynamical quantities.

This paper presents a detailed study of the microscopic nature of activated mechanisms in *a*-Si. The method that we have used is the activation-relaxation technique (ART), introduced by us a few years ago.[4] Here, we apply it to an empirical model of amorphous silicon as described by a modified Stillinger-Weber potential.[5] The activation-relaxation technique allows one to concentrate on the activated mechanisms that are responsible for most of the dynamics below melting. We have already reported a first stage of this study in a recent Letter,[6] where we concentrated on only those mechanisms involving no coordination defects.

Here we look at a wider spectrum of mechanisms, with a special emphasis on the diffusion of coordination defects.

This paper is organized as follows. In Sec. II, we describe the activation-relaxation technique and give the details of the simulations that result in the data base of events. Next, in Sec. III, we present the results extracted from this data base. Because this type of work is rather new, we also discuss the analysis of the data in some detail. The results contain both a global analysis and a more detailed topological classification.

II. METHOD OF GENERATION OF THE EVENT DATABASE

In this article, we concentrate on identifying and classifying activated mechanisms that are responsible for the relaxation and diffusion in amorphous silicon. This is done using the activation-relaxation technique (ART), an energy-landscape method, that searches for barriers and new states in complex landscapes.

As we shall see, the results we obtain are in general agreement with many of the experimental results mentioned above and provide some bounds on the type of mechanisms that can take place in *a*-Si. Of course, empirical potentials have strong limitations, especially far away from the equilibrium position for which they are developed. Without giving too much weight to the exact numerical values of the activation energies, it is nevertheless possible to give a first broad picture of the wide variety of mechanisms that can be associated with diffusion and structural relaxation. To go beyond the results presented below, it will be generally necessary to use more accurate interactions such as tight-binding or plane-wave methods.

A. Sampling one event with ART

The aim of ART is to sample minimum-energy paths, starting in a local energy minimum, passing through a first-order saddle point (where the minimum-energy path has its highest point), and leading to another local energy minimum.

PRB <u>61</u>   1898

ART does this in three stages: leaving the so-called ''harmonic well,'' convergence to the saddle point, and convergence to the new minimum. The last stage, relaxation to a local energy minimum, is straightforward and can be achieved by a wide range of standard minimization techniques, for instance the conjugate gradient (CG) method.[7] The first two stages represent the activation to a saddle point and are specific to ART. As the end conditions of the first stage (leaving the harmonic well) are set by the actual implementation of the second stage (finding the saddle point), we will discuss these two stages in reversed order.

The second stage is convergence to a first-order saddle point. At such a saddle point, the gradient of the energy is by definition zero in all directions, and the second derivative of the energy is positive in all directions but one. The single direction with negative curvature is that along which the minimum-energy path proceeds. Within ART, we make the assumption that the direction of the minimum-energy path in the saddle point and the direction towards the original local energy minimum have a significant overlap, i.e., that their dot product is significantly nonzero. If this assumption holds, a modified force field can be introduced in which the saddle point is a minimum.[8] This field is defined by the force $\mathbf{G}$

$$\mathbf{G} = \mathbf{F} - [1 - \alpha/(1 + \Delta x)](\mathbf{F} \cdot \hat{\mathbf{x}})\hat{\mathbf{x}}, \qquad (1)$$

where $\mathbf{F}$ is a $3N$-dimensional force vector obtained from the first derivative of the potential energy, $\Delta\mathbf{x}$ is the displacement vector from the minimum, and $\alpha = 0.15$ a parameter determining how fast the motion is to the saddle point. In this second stage, the redefined force $\mathbf{G}$ is followed iteratively, usually along conjugate directions, starting from just outside the harmonic well around the original local energy minimum. Ideally, this process would bring configuration directly to the saddle point and stop there, but because the projection is an approximation of the valley, the configuration passes in the vicinity of saddle point without halting. We, therefore, stop the activation as soon as the component of the force $\mathbf{F}$ projected onto the displacement $\Delta\mathbf{x}$ changes sign, an indication that a saddle point has just been past. At that point, the activation is stopped, the configuration stored as the activated configuration and we move to the relaxation. A more accurate convergence to the saddle point can be obtained by following directions determined by the eigenvectors of the dynamical Hessian,[9] but this is too costly for the system size of interest here.

Most saddle points, even those belonging to energetically favorable minimum-energy paths, cannot be reached by following this redefined force $\mathbf{G}$ from a point well inside the harmonic region, i.e., the region of the energy landscape that is well approximated by a high-dimensional parabola centered on a local minimum. We refer the reader to Ref. 10 for a detailed discussion of the origin of this problem and just describe our algorithm. We thus have to make sure that the configuration has left the harmonic well before following $\mathbf{G}$. This first stage is implemented as follows. In a local energy minimum configuration, a few atoms and their nearby neighbors are displaced randomly. The total displacement is small, typically 0.01 Å, and serves to create a nonzero force. At this point, the force will mostly point back to the minimum, and the component of the force, parallel to the displacement, will dominate the perpendicular components. However, we then increase the displacement from the original minimum until this no longer holds, and consequently we are outside the harmonic region. At that point, we can start the second stage of the activation and follow $\mathbf{G}$.

B. Generating the database

The database of events that we use in the current manuscript is generated as follows. The energy landscape is described by the Stillinger-Weber potential,[5] modified as described below. This empirical interaction includes a two-body and a three-body interaction

$$E = \sum_{\langle ij \rangle} V(r_{ij}) + \sum_{\langle ijk \rangle} V(r_{ij}, r_{ik}, \theta_{jik}), \qquad (2)$$

where the brackets $\langle$ and $\rangle$ indicate that each bond or angle is only counted once; the two-body potential is

$$V(r_{ij}) = \epsilon A(B r_{ij}^{-p} - 1) \exp[(r_{ij} - a)^{-1}] \qquad (3)$$

and the three-body potential is

$$V(r_{ij}, r_{ik}, \theta_{jik}) = \epsilon\lambda(\cos\theta_{jik} + \tfrac{1}{3})^2 \exp[\gamma(r_{ij} - a)^{-1}]$$
$$\times \exp[\gamma(r_{ik} - a)^{-1}]. \qquad (4)$$

The numerical values for the parameters are $A = 7.050$, $B = 0.6022$, $p = 4$, $a = 1.80$, $\lambda = 31.5$, $\gamma = 1.20$, $\sigma = 2.0951$ Å, and $\epsilon = 2.1682$ eV; this set is identical to that used by Stillinger and Weber except for λ, which has been increased by a factor of 1.5 in order to provide a more appropriate structure for a-Si.[4,10,11] Recent work on fracture underlines the fact that none of the available empirical interaction potentials describe silicon exactly.[12] This is particularly the case for energy barriers and density of defects; trends, more than exact values, are therefore what we are looking for here.

We report here on results obtained from three independent runs. Each initial 1000-atom cell is constructed by a random packing in a large cubic cell. This configuration is then minimized at zero pressure to a nearby minimum state. ART is then applied iteratively with a Metropolis temperature of 0.25 eV in order to bring the configuration to a well-relaxed amorphous state; we consider that a system is ''well-relaxed'' when the energy does not decrease significantly over hundreds of events. This takes place after about 5000 trial events, with a success rate slightly above 65%.

After reaching a plateau in energy, for each event we store the initial minimum configuration, the saddle-point configuration, and the final minimum configuration. Over the three independent runs, we collected a set of 8106 events. Figure 1 shows the radial distribution function for run C at the beginning ($C1$) and end of the data acquisition run, 5000 trial events later ($C5000$). Although radial distribution functions cannot discriminate easily between realistic and nonrealistic structure,[13] the one obtained here is in good agreement with experimental data.[14]

Table I shows the structural properties of these two networks. A third of the bonds, involving 42% of the atoms, have been changed and yet the total energy and structural properties are almost unchanged. This is an indication that
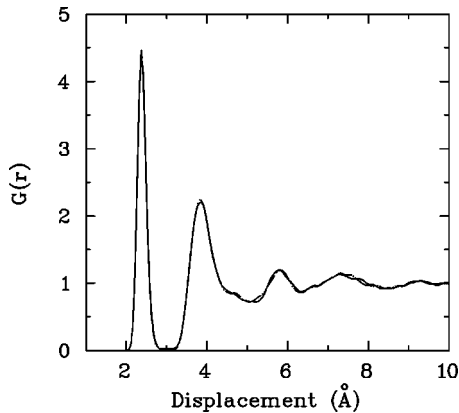
FIG. 1. Smoothed radial distribution function for configurations $C1$ (solid line) and $C5000$ (dashed line).

the configuration, through a sequence of events, has evolved considerably on an almost constant energy surface.

The bond-angle distribution and coordination is comparable with the best networks as obtained with realistic potentials.[11,15] A comparison with experiment is more difficult. Experimental works on amorphous silicon samples prepared by ion-bombardment report that homogeneous samples of a-Si, without voids, have a density about 1.8% lower than c-Si.[16,17] Recent high-Q x-ray diffraction measurements on similarly prepared samples show that well-relaxed a-Si could have an average coordination as low as 3.88, much below the 4.0 generally considered to be appropriate for ideal a-Si.[18] The authors of this paper conclude that the high density of dangling bonds should be responsible for the lower density of these samples. This analysis is not supported by our simulation, which leads to cells with a density as low as 7% below that of the crystal, while keeping the number of defects *lower* than that seen in this experiment. Clearly, more work needs to be done to clarify this situation, especially since the 12% of dangling bonds seen by high-Q diffraction is at least an order of magnitude higher than what can be expected from either differential scanning calorimetry (1% defects) and electron-spin resonance measurements (0.04% defects).[2] These results also contrast with *ab initio* and tight-binding computer simulations, which tend to find higher coordination, often above 4.0.[19] The origin of this discrepancy

TABLE I. Structural properties of configurations $C1$ and $C5000$, the first and last structures used during the data collection in run C: the energy per atom in electron Volt, the distribution of coordination using a cut off at 3.05 Å, the average bond angle and the width of the related distribution. The two configurations differ by 33% in their bonding and 42% of the atoms have changed their neighbor list.

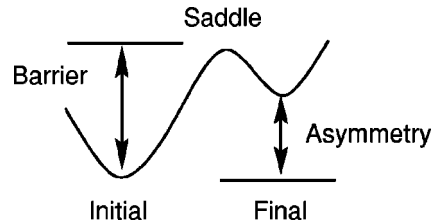|	$C1$	$C5000$
Energy (eV)	-3.903	-3.918
three-folds	0.043	0.035
four-folds	0.948	0.960
five-folds	0.009	0.005
$\langle r \rangle$	3.966	3.97
θ	109.27	109.32
$\Delta \theta$	10.04	9.74

FIG. 2. The energy barrier and asymmetry in a schematic event as created by the activation-relaxation technique.

is hard to identify at the moment but it can be due to a combination of inaccurate interactions and/or the differences in time and lengths scales between simulations and experiments. In the case of our simulations, the stability of the configurations after 5000 trial events suggests that we have reached some type of thermalization for this given interaction potential.

III. GENERAL PROPERTIES OF EVENTS

A. Asymmetry, activation energy, and displacement

The events can first be classified in term of three energies: the energy asymmetry, the activation energy, and the total atomic displacement (see Fig. 2.) The simplest quantities to use for the classification of events are the barrier and asymmetry energies. In Ref. 6, we give the distribution of these two quantities for the full set of 8106 events. Both distributions are wide and relatively smooth. To push further the analysis, it is useful to establish a first classification based on topological properties of the network.

The radial distribution function of relaxed a-Si goes to zero between the first and second neighbor. The middle of this region between first and second neighbor lies at around 3.05 Å. This allows us to establish a clear definition of nearest-neighbor bonds between atoms. Structural properties of the first and last minimum-energy configurations of run C in our database are listed in Table I; we find similar numbers for runs A and B. Most atoms that change neighbors in an event are fourfold coordinated both before and after. We discern three topological classes of events: if *all* atoms involved in an event keep their coordination unchanged between the initial and final state, we term it a *perfect* event; if topological defects change place during an event, but their total number is conserved, we have a *conserved event*, which describes defect diffusion; the remaining events are called creation/annihilation events.

The exact details of the number of each class of events depends slightly on the cut-off radius between first and second neighbors; although low-energy configurations have a clear gap between first- and second-neighbor peaks in the radial distribution function, many saddle and some high-energy final configurations show structure in this gap. For consistency, we have chosen a fixed cut-off at 3.05 Å for all our analysis; the topological classification of some events might be affected by these parameters but the overall conclusions are not sensitive to the fine tweaking of that value.

In a previous letter, we have discussed in some detail the class of perfect events (802 events).[6] The bulk of our database comprises creation/annihilation events, with 5325 events, but until now we did not succeed in revealing inter-

FIG. 4. Distribution of total displacement at the barrier (dashed line) at the new minimum (solid line) for conserved events.
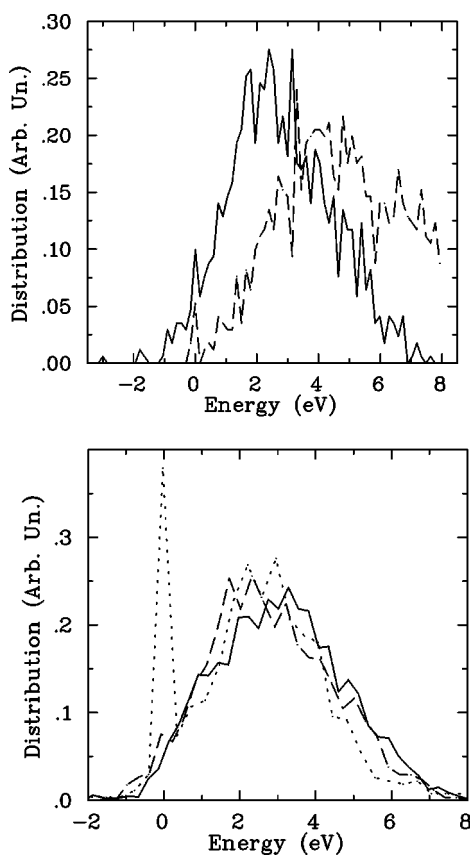
FIG. 3. Top: Distribution of the energy barrier (dashed line) and energy assymetry (solid line) for the 1979 conserved events. Bottom: Comparison of the renormalized asymmetry energy distribution for the conserved (dashed line) and the perfect events (dotted line) and all the others (solid line).

esting characteristics from these. In this paper, we focus on the 1979 conserved events in our database, describing directly the diffusion of defects without the creation or annihilation of coordination defects.

As already mentioned, we produced 1979 conserved events, i.e., events where the number of coordination defects is identical in the initial and final state. The distribution of barriers and minimum to minimum energy differences is shown in Fig. 3(a). The front of the barrier distribution peaks at about 4.5 eV while the asymmetry peaks at about 2.1 eV. This distribution is very similar to the total distribution shown in Fig. 1 of Ref. 6. In fact, one of the most striking results we obtain is that the distribution of barriers and asymmetry is almost independent of the subset of events we select. The bottom box of Fig. 3, for example, compares the asymmetry distribution for the three classes of events: perfect, conserved, and creation/annihilation. Except for the peak at 0 eV in the case of perfect events, involving atomic exchanges without modification of the overall topology of the network, the three distributions fall almost on top of each other at low asymmetry. The maximum of each distribution is slightly shifted, however, with peaks at about 2.3 eV for the conserved events, 2.5 eV for the perfect events and 3.2 eV for creation/annihilation events.

The bias towards higher energies in the asymmetry distribution is expected: the distribution includes all attempted events, and not 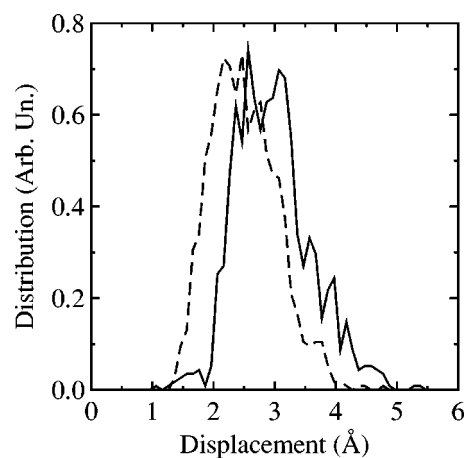just those that are accepted; since the run is started in an already well-relaxed configuration, most events lead to higher energy configurations.

A similar insensitivity can be seen with the activation barriers. Although the precision on the barrier height is about 0.5 eV within the modified-force approximation, we can still say something about activation. Figure 3 also plots the distribution of barriers. It peaks at about 4.0 eV. Taking into account the weaknesses of the empirical potential and the uncertainty on the barrier, this result is not inconsistent with experimental measurement. Shin and Atwater[20] conclude, based on conductivity measurements, that the activation-energy spectrum extends from as low as 0.25 eV to about 2.8 eV, supposing that a prefactor (entering logarithmically in the relation) is of order 1. Using isothermal calorimetry, Roorda et al.[2] find relaxation with a characteristic time of about 110 s between 200 and 500 C, also indicating a high-activation barrier. Moreover, these results seem to depend only weakly on the method of preparation (vacuum evaporation or ion implantation) and are limited by the fact that above 500 C the samples tend to crystallize. Both results are therefore also consistent with a continuous distribution of activation barriers.

The tail of the distribution goes much beyond experimental values, and extends past 20 eV. Although such mechanisms are clearly unphysical, they underscore the fact that ART does not suffer from slowing down as the height of the barrier increases. This method is perfectly at ease with barriers of 0.1 eV as well as those of 25 eV. In the rest of this paper, we will concentrate on events with the 1147 more physical barriers of less than 8 eV.

Figure 4 shows the histogram of the total displacement, defined as the square root of the sum of the square of each single-atom displacement, for these conserved events with a barrier of less than 8 eV. There is again little structure in the distribution. We note that the average displacement to the saddle point is shorter than that to the new minimum. Based on preliminary simulations in other materials, this trend, although intuitively reasonable, is not always present and might be indicative of certain types of activation; more work remains to be done to clarify this issue.

B. Volume expansion/contraction per event

If is often suggested that there should be correlation between the energy of an event and its size. This immediately

raises the question as to whether mechanisms by which the structure rearranges itself are local or nonlocal.

Based on the observation that isothermal heat release curves obey bimolecular reaction kinetics and that the ion-beam-induced derelaxation scales with the density of displaced atoms due to the ion bombardment and appears to be independent of electronic energy-loss mechanisms, Roorda[2] concludes that point-defect annihilation should control the structural relaxation. It remains unclear, however, whether this means the actual removal of defects or simply a clustering or a passivation by hydrogen atoms. A similar relaxation (to within a factor 2) of ion-bombarded c-Si and a-Si suggests that both materials have similar relaxation mechanisms but not necessarily identical. This similarity would point towards relatively local mechanisms of defect diffusion and relaxation since at this length scale, crystalline and amorphous materials resemble each other closely.

Based on EPS data however, Muller *et al.* suggest that from 1000 to 10 000 atoms have to move marginally in order to enable a single dangling-bond defect to anneal.[21] This would be, at least qualitatively, in agreement with x-ray photoemission spectroscopy (XPS) measurements that suggests that the formation of dangling bonds in a-Si:H under exposure to light is also accompanied by long-range structural rearrangements of the amorphous network,[22] but it is in clear disagreement with the conclusion of Roorda *et al.* mentioned above. The annealing mechanism suggested by this group, for example, is mutual annihilation of low- and high-density defects—vacancy/interstitial. Roorda *et al.* propose defects similar to that of c-Si but not necessarily identical.[2] Mössbauer experiments with Sn suggest that vacancies exist also in a-Si.[23] Part of the difficulty in assessing more clearly the type of defects involved in relaxation and diffusion is that amorphous silicon crystallizes at about 500 C, rendering studies of selfdiffusion very difficult.[24]

Because it is not always clear what size means, we consider here three definitions: number of atoms, total displacement and local-density deformations.

The size of events is usually related to the number of atoms involved in the rearrangement of the network, i.e., the number of atoms that are displaced more than a threshold distance r_c. In Fig. 5, we plot the number of atoms involved as a function of r_c, for the conserved and the full set of events. A local topological rearrangement will generally push the surrounding atoms outwards, or occasionally pull them slightly inwards. The distance Δr over which the surrounding atoms are pushed away (pulled inwards) will, because of elasticity arguments, scale with the distance r from the rearrangement as $\Delta r \sim r^{-2}$, for sufficiently large r. Alternatively, this can be rewritten as $\Delta r \cdot r^2 = V_e$, where V_e is a constant volume independent of the distance r. The distance over which the atomic displacement Δr exceeds a threshold displacement r_c is then equal to $r = \sqrt{V_e / r_c}$, and the number of atoms displaced more than r_c will then scale with r_c as $N_e \sim V_e^{3/2} r_c^{-3/2}$. Figure 5 shows that this scaling holds in the region where $0.1 < r_c < 1.0$ Å and $N_e \ll N$. Selecting a threshold at 0.1 Å the lower bound but also the typical vibration displacement at room temperature in Si, we find that, on average, about 50 atoms are involved in an event, clearly beyond the very local mechanism but well below the highest numbers proposed.
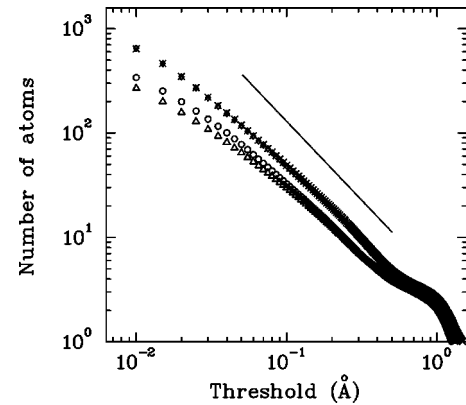

FIG. 5. Number of atoms displaced by a minimum threshold distance. The triangles and the X's are for saddle and new minimum positions averaged over all events; the circles and diamonds are averaged over conserved events. In the case of activation, both distributions fall exactly on top of each other and it is hard to distinguish the X's from the diamonds. The solid line corresponds to the elasticity scaling, $N \sim r^{-1.5}$ as discussed in the text.

The size of the events can thus be measured also without the introduction of a threshold distance, by measuring $V_e = \Delta r \cdot r^2$, averaged over some range of r. Figure 6 shows the correlation between the event volume and the energy barrier and asymmetry. The figure shows that most proposed events tend to expand the sample locally by about $V_e \sim 1$ Å^3. More-
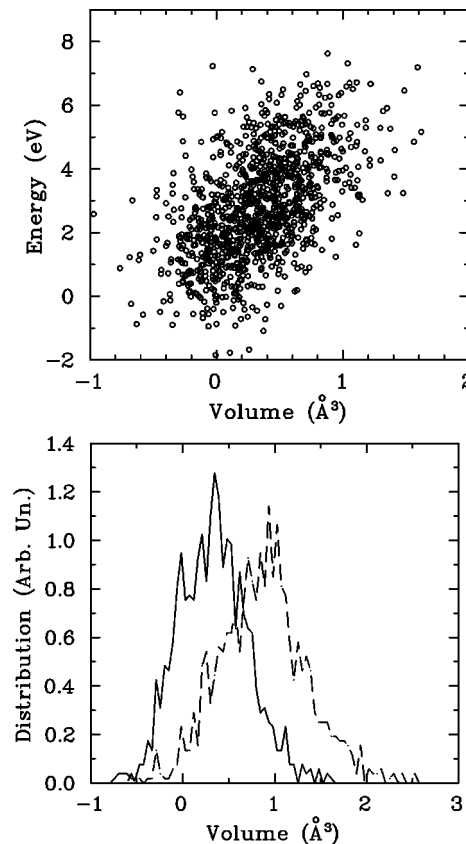

FIG. 6. Top: Asymmetry energy as a function of the volume of the event (as defined in the text) for conserved events. Bottom: Distribution of the volume of events for conserved events at the saddle point (dotted line) and at the new minimum (solid line).
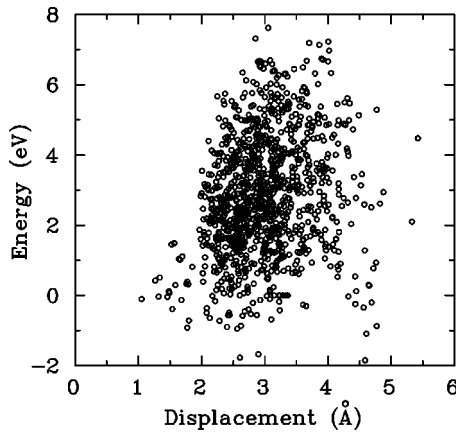
FIG. 7. Asymmetry energy as a function of total displacement for the conserved events.
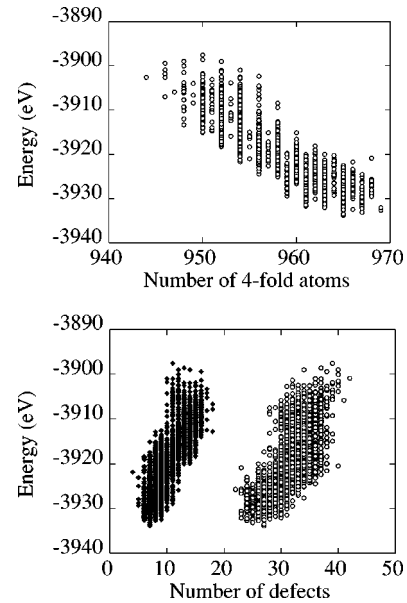

FIG. 8. Top: Total energy as a function of the number of four-fold atoms; bottom: total energy as a function of the number of three-fold (open circle) and five-fold (full diamonds) for all events.

over, although scattered considerable, the data suggest a linear relation between the energy and the volume expansion with about 4 eV per $Å^3$.

We can also search for correlations between the total displacement and the asymmetry energy, which could relate the diffusion length with the energy. This is plotted, for conserved events, in Fig. 7; there is little correlation. A similar negative result is obtained if we look at the correlation between the displacement and the activation energy.

The picture that emerges from these three approaches is that events are relatively localized, involving around 50 atoms, and require some local expansion to take place, as would be expected. Correlations between the size of events and the energy are difficult to establish due, in large part, to the wide spread of local environment typical of disordered systems. These results can be used to put bounds on models of diffusion and relaxation in amorphous silicon.

C. Energetics of coordination defects

Weak bonds and coordination defects form another recurring theme in the study of dynamics and relaxation in a-Si. In this section, we discuss their properties in the sub-set of conserved events. The number of bonds broken/created at the saddle point is 3.7 ± 1.4 and 3.4 ± 1.4 with bond lengths of 2.43 ± 0.09 and 2.62 ± 0.12 Å. At the final point, it is 4.3 ± 1.6 (equal number of bonds created and broken for a conserved event) with respective bond lengths of 2.46 ± 0.09 and 2.55 ± 0.10 Å.

These numbers are very similar to those obtained by concentrating on perfect events.[6] This reflects one of our main conclusions: that correlation between different properties of the events is weak. If the bond length of the resulting states is typically longer than that of the initial configuration, it is simply because the final configurations have typically a significantly higher energy. There is no preference for a single-stretched bond; it is the medium-range strain that matters.

One would expect a relation between relaxation and defect annihilation, but how strongly linked these two are is not clear *a priori*. Relatively little is know directly.[25] To a first approximation, the total energy should follow the density of defects.[26] Because of the similarity between crystalline and amorphous Si, Roorda *et al.* concluded that relaxation occurs through defect annihilation.[2] Polman *et al.* find that Cu dif-

fusion in annealed a-Si is 2 to 5 times faster than in nonannealed samples; this increase in diffusion might indicate a decrease in defects, trapping the Cu.[24]

We see a certain correlation between defects and total energy as plotted in Fig. 8(a). The distribution of energy for a given number of defects is wide, going from 12 eV for 35 defects to about 25 eV for 50 defects. Looking at the correlations of the energy with specific type of defects, we find much smaller impacts, with significant distribution in the total energy for a given number of three-fold or five-fold defects as is shown in the bottom panel for Fig. 8.

Clearly, therefore, the definition of defects must also include strained environment and not just the coordination defects mentioned here—relaxing some highly strained ring might require the creation of a bond defect. Once again, the situation is much less clear than is generally thought. We must emphasize here that for less relaxed samples, the correlation between energy and the number of coordination defects is much better.

D. Topological classification

To go beyond the scalar picture given above, we need to consider in more detail the nature of the topological changes. The classification scheme applied here is an extension to the classification scheme that we used for the perfect events in an earlier letter.[6] All atoms that change their neighbors are alphabetically labeled. The topological change is determined by specifying the list of all bonds before the event, and of all bonds after.

For perfect events, there are as many bonds before as after the event, and moreover, the set of all these bonds can always be organized into a ring of alternating created and destroyed bonds. This ring can be represented by the sequence of atoms visited. For instance, in event *abacbd*, the bonds before and after the event are *ab, ac, bd*, respectively *ba, cb, da*. Thus, bonds *ac* and *bd* are replaced by *ad* and *bc*, while

TABLE II. Most common events for low energy conserved events. The first column gives the classification label in terms described above. The second and the third columns refer to the number of events carrying this label and the number of topological defects—typically dangling bonds—displaced in the event, respectively. The last column, finally, gives a topological indication of how far the defect diffuses. A local jump brings a defect from one atom to its near neighbor; nonlocal events will involve jumps to the second, third, or even fourth neighbor.

Topology	Occurrence	No. defects	Local/nonlocal
abacadefbfgbedc	2	1	local
abacadefegfbedc	2	1	local
abacb	9	1	local
abacbdaeb	5	1	local
abacbdaebfagb	6	1	local
abacbdaebfagc	2	1	local
abacbdaebfbgf	4	1	2nd neighbor
abacbdaec	8	1	local
abacbdaef	6	1	local
abacbdaefageg	2	1	local
abacbdbed	5	1	2nd neighbor
abacbdbedcfcfg	6	1	local
abacbdbedcfcgdf	2	1	local
abacbdbefegfdg	4	1	local
abacbde	3	1	2nd neighbor
abacdcedb	8	1	local
abacbdedfeb	5	1	local
abacdcedbfdfe	2	1	2rd neighbor
abacdcedbfdfg	8	1	3rd neighbor
abacdcedbfdfgeg	4	1	3rd neighbor
abacdcedfcb	4	1	local
abacdcefbfgbechdi	3	1	3rd neighbor
abacdebefbdcg	11	1	2nd neighbor
abacdefegfdcb	3	1	local
abc	9	1	local
abcde	2	1	4th neighbor
abcbdcebf	7	1	local
abcbdcebfcg	5	1	3rd neighbor
abcdc.ec.fdg.ehi	1	4	2nd neighbor

bond *ab* is present both before and after the event. Many equivalent rings exist, but the convention of always using the alphabetically lowest label makes this classification unique.

If the event is not perfect, this classification scheme has to be modified. In case a single bond (or dangling bond) jumps from one atom to another, the set of bonds does not form a closed ring, but an open chain of alternating bonds before and after the event; the same classification scheme can still be used, with the note that the first and last atom are not bonded. It also happens that the event comprises a series of bond exchanges, which are in disconnected regions (typically still nearby-interacting via the strain field). For such events, we introduce the concept of ''ghost bonds'' (represented by a dot in the label), that are added to either the set of bonds before or after the event.

Using this topological analysis, we can have a first crack at the events. 1148 events in our database have an activation
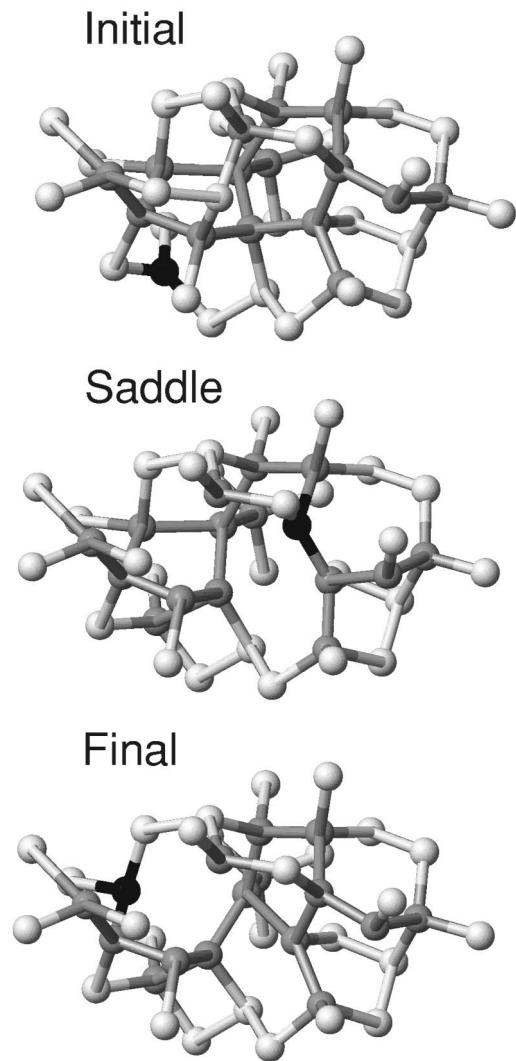

FIG. 9. Event of type ''*abcbdce*'' in a 1000-atom cell. Barrier: 4.3 eV, Asymmetry: 0.3 eV, total displacement 1.8 Å, four bonds broken and four created. The dark atom carries the dangling bond as it jumps over 2 neighbours; the gray atoms are either changing their local environment or moving by more than 0.1 Å; the white atoms are there to give a better representation of the network.

barrier of less than 8 eV, the other events might be considered unphysical. Of these, 447 are too complicated (involving too many defects or too many disconnected regions) to be analyzed, leaving 701 labeled events.

For conserved events, there are no dominant labels, contrary to what is found for perfect events where three labels account for 85% of the events. Such diversity underscores the difficulty in trying to identify mechanisms and relating them to experimental information. Clearly, the dynamics of defects in amorphous silicon is much more complicated than is usually thought.

In the large set of labels, an often occurring theme is a ring of bonds corresponding to the Wooten-Winer-Weaire (WWW) bond-exchange mechanism,[27,28] which in our classification scheme has the label *abacbd*. We find that up to two WWW moves can take place in a single event. This rearrangement changes the local ring structure and redistributes the strain, affecting the jump barrier seen by the dangling bond.

After removal of all these rings from the events as such, what remains is often a single coordination defect that jumps to a 1st, 2nd, or higher neighbor. Table II presents a partial list of such labels. It is remarkable that the diffusion of coordination defects requires, in general, a topological rearrangement more complex than one would expect from the displacement of the bonds. Only nine events are of the *abc* type, the smallest rearrangement possible for the motion of a bond.

Other events involve longer jumps, at least in topological terms. The *abacbde*, for example, reflect this type of behavior. We show one such event in Fig. 9. Very few of the classified events displace more than one defect. (It could be that in the non-classified events this situation occurs more often.)

IV. CONCLUSIONS

Based on an extensive list of events in *a*-Si, representing a wide range of characters, we can provide a general overview of the nature of the microscopic mechanisms responsible for the diffusion of topological defects in this material. To do so, we have concentrated on a class of events that involve the displacement of coordination defects while keeping their overall number constant.

Analyzing a wide range of structural and topological properties of these events we find that: (1) In a well-relaxed sample, there is little correlation between the number of defects and the total energy; the relaxation of strain can take place in more subtle ways, sometimes involving the creation of topological defects. (2) Taken into account the use of an empirical potential, the activation barriers are in agreement with experimental value. (3) We find little correlation between the activation barrier or the asymmetry and the deformation of the network, either in terms of the number of atoms involved or the total displacement; the energy is best described in term of the volume of an event. (4) A topological analysis of the conserved events show an unexpected richness; we find literally hundreds of different mechanisms that cannot easily be put in a few classes. As a rule, the Wooten-Weaire-Winer bond exchange mechanism, dominant for perfect events, still plays a major role. Defect diffusion is often local, with coordination defects jumping from one atom to a neighbor, but it can also go as far the fourth neighbor, in a chainlike fashion.

These results can be used to put bounds on models of diffusion and relaxation in amorphous silicon. For example, the Fedders and Branz model for *a*-Si:H (Ref. 29) states that (1) relaxing the defect structure often requires several atoms to move simultaneously, (2) only by cooperative motion do the position changes lower or conserve the total energy, (3) the size of the barrier generally increases with the number of atoms that must move simultaneously. Our results support points (1) and (2) but not (3).

This study represents only a first step in the study of microscopic activated mechanisms in *a*-Si. More work remains to be done to converge barriers using more accurate interaction potentials. It is important also to try to connect some of these results with hard experimental numbers, a challenge both for theorists and experimentalists. Already, however, we can see that the dynamics of disordered materials promises to be much more complicated than was thought before.

*Electronic address: mousseau@helios.phy.ohiou.edu

†Electronic address: barkema@phys.uu.nl

[1] X. Liu, B.E. White, Jr., R.O. Pohl, E. Iwanizcko, K.M. Jones, A.H. Mahan, B.N. Nelson, R.S. Crandall, and S. Veprek, Phys. Rev. Lett. **78**, 4418 (1997).

[2] S. Roorda, W.C. Sinke, J.M. Poate, D.C. Jacobson, S. Dierker, B.S. Dennis, D.J. Eaglesham, F. Spaepen, and P. Fuoss, Phys. Rev. B **44**, 3702 (1991).

[3] N. Mousseau and L.J. Lewis, Phys. Rev. Lett. **78**, 1484 (1997).

[4] G.T. Barkema and N. Mousseau, Phys. Rev. Lett. **77**, 4358 (1996).

[5] T.A. Weber and F.H. Stillinger, Phys. Rev. B **32**, 5402 (1985).

[6] G.T. Barkema and N. Mousseau, Phys. Rev. Lett. **81**, 1865 (1998).

[7] W.H. Press, S.A. Teukolsky, W.T. Vetterling, and B.P. Flannery, *Numerical Recipes* (Cambridge University Press, Cambridge, 1988).

[8] We have recently relaxed this assumption by introducing some trailing in the algorithm. Such modification has been significant in metallic glasses and polymers but has not changed the results for *a*-Si.

[9] J.P.K. Doye and D.J. Wales, Z. Phys. D **40**, 466 (1997).

[10] N. Mousseau and G.T. Barkema, Phys. Rev. E **57**, 2419 (1998); Comput. Sci. Eng. **1**, 74 (1998).

[11] K. Ding and H.C. Andersen, Phys. Rev. B **34**, 6987 (1986).

[12] J.A. Hauch, D. Holland, M.P. Marder, and H.L. Swinney, Phys. Rev. Lett. **82**, 3823 (1999).

[13] N. Mousseau and L.J. Lewis, Phys. Rev. B **56**, 9461 (1997).

[14] G. Etherington, A.C. Wright, J.T. Wenzel, J.C. Dore, J.H. Clarke, and R.N. Sinclai, J. Non-Cryst. Solids **48**, 265 (1982).

[15] J.F. Justo, M.Z. Bazant, E. Kaxiras, V.V. Bulatov, and S. Yip, Phys. Rev. B **58**, 2539 (1998).

[16] J.S. Custer, M.O. Thompson, D.C. Jacobson, J.M. Poate, S. Roorda, W.C. Sinke, and F. Spaepen, Appl. Phys. Lett. **64**, 437 (1994).

[17] D.L. Williamson, S. Roorda, M. Chicoine, R. Tabti, P.A. Stolk, S. Acco, and F.W. Saris, Appl. Phys. Lett. **67**, 226 (1995).

[18] K. Laaziri, S. Kycia, S. Roorda, M. Chicoine, J.L. Robertson, J. Wang, and S.C. Moss, Phys. Rev. Lett. **82**, 3460 (1999).

[19] For a set of references, see L.J. Lewis and N. Mousseau, Comput. Mater. Sci. **12**, 210 (1998).

[20] J.H. Shin and H.A. Atwater, Phys. Rev. B **48**, 5964 (1993).

[21] G. Müller, G. Krötz, S. Kalbitzer, and G.N. Greaves, Philos. Mag. B **69**, 177 (1994).

[22] D.P. Masson, A. Ouhlal, and A. Yelon, J. Non-Cryst. Solids **190**, 151 (1995).

[23] Z.N. Liang, L. Niesen, G.N. van den Hoven, and J.S. Custer,

Phys. Rev. B **49**, 16 331 (1994).

[24] A. Polman, D.C. Jacobson, S. Coffa, and J.M. Poate, Appl. Phys. Lett. **57**, 1230 (1990).

[25] C.A. Volkert, J. Appl. Phys. **74**, 7107 (1993).

[26] S. Wagner, H. Gleskova, and J-I. Nakata, J. Non-Cryst. Solids **198-200**, 407 (1996).

[27] F. Wooten, K. Winer, and D. Weaire, Phys. Rev. Lett. **54**, 1392 (1985).

[28] F. Wooten and D. Weaire, Solid State Phys. **40**, 1 (1987).

[29] P.A. Fedders and H.M. Branz, J. Non-Cryst. Solids **190**, 142 (1995).